Neurobiology:

Estrogen Receptor β and Its Domains Interact with Casein Kinase 2, Phosphokinase C, and *N*-Myristoylation Sites of Mitochondrial and Nuclear Proteins in Mouse Brain

Vijay Paramanik and Mahendra Kumar Thakur

J. Biol. Chem. 2012, 287:22305-22316.
doi: 10.1074/jbc.M112.351262 originally published online May 7, 2012

THE JOURNAL OF BIOLOGICAL CHEMISTRY VOL. 287, NO. 26, pp. 22305–22316, June 22, 2012

Estrogen Receptor β and Its Domains Interact with Casein Kinase 2, Phosphokinase C, and *N*-Myristoylation Sites of Mitochondrial and Nuclear Proteins in Mouse Brain*[S]

Received for publication, February 9, 2012, and in revised form, May 1, 2012 Published, JBC Papers in Press, May 7, 2012, DOI 10.1074/jbc.M112.351262

Vijay Paramanik and Mahendra Kumar Thakur[1]

From the Biochemistry and Molecular Biology Laboratory, Centre of Advanced Study, Department of Zoology, Banaras Hindu University, Varanasi-221 005, India

Background: Estrogen receptor β and its domain interact with a host of brain mitochondrial and nuclear proteins.
Results: Estrogen receptor β interacting brain mitochondrial and nuclear proteins have consensus motifs.
Conclusion: Estrogen receptor β interacts with casein kinase 2, phosphokinase C, and *N*-myristoylation sites present in mitochondrial and nuclear proteins.
Significance: This might be useful to regulate estrogen-dependent gene regulation in brain for therapeutics.

The localization of estrogen receptor (ER)β in mitochondria suggests ERβ-dependent regulation of genes, which is poorly understood. Here, we analyzed the ERβ interacting mitochondrial as well as nuclear proteins in mouse brain using pull-down assay and matrix-assisted laser desorption ionization mass spectroscopy (MALDI-MS). In the case of mitochondria, ERβ interacted with six proteins of 35–152 kDa, its transactivation domain (TAD) interacted with four proteins of 37–172 kDa, and ligand binding domain (LBD) interacted with six proteins of 37–161 kDa. On the other hand, in nuclei, ERβ interacted with seven proteins of 30–203 kDa, TAD with ten proteins of 31–160 kDa, and LBD with fourteen proteins of 42–179 kDa. For further identification, these proteins were cleaved by trypsin into peptides and analyzed by MALDI-MS using mascot search engine, immunoprecipitation, immunoblotting, and far-Western blotting. To find the consensus binding motifs in interacting proteins, their unique tryptic peptides were analyzed by the motif scan software. All the interacting proteins were found to contain casein kinase (CK) 2, phosphokinase (PK)C phosphorylation, and *N*-myristoylation sites. These were further confirmed by peptide pull-down assays using specific mutations in the interacting sites. Thus, the present findings provide evidence for the interaction of ERβ with specific mitochondrial and nuclear proteins through consensus CK2, PKC phosphorylation, and *N*-myristoylation sites, and may represent an essential step toward designing selective ER modulators for regulating estrogen-mediated signaling.

Estrogen receptor (ER),[2] a ligand-activated transcription factor belonging to the nuclear receptor superfamily, has two main types: ERα and ERβ. These receptors are localized intracellularly and following ligand binding, they regulate a large number of estrogen responsive genes (1, 2). They are also present in the plasma membrane and involved in many rapid, non-genomic effects via several signaling pathways (3, 4). In addition, ERβ is located in the mitochondria of estrogen target cells, including human breast cancer MCF-7 cells (5, 6). ER interacts with a large number of factors such as steroid receptor coactivator (SRC)-1 (7), glucocorticoid receptor-interacting protein (GRIP)-1 (8), transcriptional intermediary factor (TIF)-2 (9), and others (10) that may activate (coactivators) or suppress (corepressors) the transcription of specific genes. Coactivators exhibit a region called helix-12 which includes NR boxes, each containing a L*XX*LL motif (where L is leucine and *X* represents any amino acid) (11), through which it interacts with ER as shown by functional *in vitro* and *in vivo* studies (12, 13). Mapping studies with corepressors reveal that the receptor interaction and repression functions are separately located toward the *C*-terminal (14).

The corepressors namely silencing mediator for retinoic acid receptor and thyroid hormone receptor (SMRT)and N-CoR have interaction motifs of short peptides comprising of 19 amino acids and 17 amino acids, respectively, with an internal signature motif (I/L)*XX*(I/V)I, which is sufficient for receptor interaction and ligand-induced dissociation. These motifs can adopt an amphipathic α-helical conformation, reminiscent of the signature motif L*XX*LL within coactivators (15). Mitochondrial localization of ERβ helps to understand the mechanism(s) of neuronal death and develop neuroprotective drugs and therapeutic strategies that can delay or prevent Alzheimer disease and other chronic neurodegenerative conditions. In the brain, estrogens exhibit multiple effects that enhance or preserve functions during pathologic circumstances such as excitotoxic-

* This work was supported by the Indian Council of Medical Research (ICMR) and Department of Biotechnology (DBT/BT/PR3593/Med/14/468/2003), Government of India (to M. K. T.) and a Senior Research Fellowship from ICMR (to V. P.).
[S] This article contains supplemental Tables S1 and S2, Figs. S1 and S2, and Materials and Methods.
[1] To whom correspondence should be addressed: Biochemistry and Molecular Biology Laboratory, Centre of Advanced Study, Department of Zoology, Banaras Hindu University, Varanasi-221 005, India. Tel.: 0542-6702521; Fax: 0542-2368174; E-mail: mkt_bhu@yahoo.com.

[2] The abbreviations used are: ER, estrogen receptor; TAD, transactivation domain; LBD, ligand binding domain; PTK, protein tyrosine kinase; NMT, *N*-myristolyltransferase; SRC, steroid receptor coactivator; TIF, transcriptional intermediary factor.

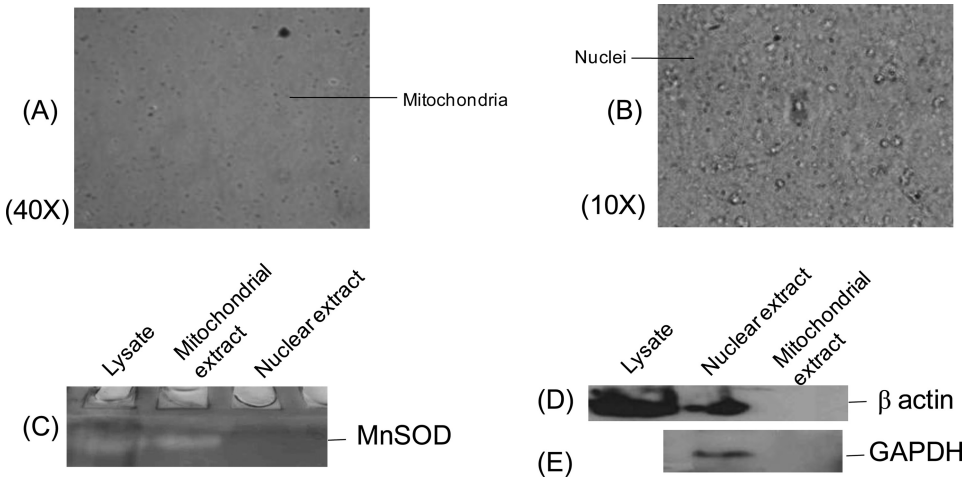

FIGURE 1. **Photograph observed under a microscope.** *A*, mitochondria; *B*, nuclei; *C*, in-gel assay showing presence of MnSoD in lysate and mitochondrial fraction and absence in nuclear fraction. *D*, immunoblotting showing presence of β-actin in lysate and nuclear fraction and absence in mitochondrial fraction. *E*, immunoblotting showing presence of GAPDH in nuclear fraction and absence in mitochondrial fraction.

ity, oxidative stress, and neurodegeneration. However, the ERβ and its domain interacting proteins and their cellular functions are poorly understood in the brain, specifically in mitochondria. Here we report the identification of ERβ, transactivation domain (TAD) and ligand binding domain (LBD)-interacting proteins from the mitochondrial and nuclear extract of the mouse brain by pull-down and matrix-assisted laser desorption ionization mass spectroscopy (MALDI-MS) followed by analysis with mascot search engine and motif search software to determine the consensus binding motifs.

EXPERIMENTAL PROCEDURES

Cloning and Expression of ERβ, TAD, and LBD

Detailed procedures are discussed in supplemental Materials and Methods. Briefly, the same procedures were followed as reported earlier (16).

Purification of Recombinant Proteins

These are discussed in supplemental Materials and Methods. Briefly, the same procedures were followed as reported earlier (17).

Interaction of ERβ, TAD, and LBD with Mitochondrial and Nuclear Extract of Mouse Brain

Purification of Mitochondria and Preparation of Mitochondrial Extract—For mitochondrial purification (18), the mouse brain was dissected on ice and rapidly minced and homogenized at 4 °C in isolation buffer (225 mM mannitol, 75 mM sucrose, 5 mM HEPES, 1 mM EGTA, 1 mg/ml BSA, pH 7.4). Then the homogenate was centrifuged at 600 × *g* for 5 min at 4 °C. The supernatant was collected and centrifuged at 9,000 × *g* for 8 min at 4 °C. Thereafter the pellet was resuspended in isolation buffer containing heparin to release the mitochondria from synaptosome and again centrifuged at 9,000 × *g* for 8 min at 4 °C. Then the brownish mitochondrial pellet was resuspended in isolation buffer and spun at 9,000 × *g* for 10 min at 4 °C. The pellet containing mitochondria was resuspended in suspension medium (isolation buffer with 0.02% w/v heparin). Before preparing extract mitochondria were observed under microscope to avoid contamination (Fig. 1). The suspension was incubated with lysis buffer containing 20 mM HEPES (pH 7.6), 25% glycerol, 420 mM NaCl, 1.5 mM $MgCl_2$, 0.2 mM EDTA, 0.5 mM PMSF, 0.5 mM DTT, 0.4 mg/ml complete EDTA-free protease inhibitor (Roche Diagnostics) and stirred for 30 min on ice. Then it was centrifuged at 25,000 × *g* for 40 min at 4 °C. The supernatant containing the mitochondrial extract was checked quantitatively by the Bradford method and qualitatively by silver staining. The purity of mitochondrial extract was checked by in gel assay of MnSOD and immunoblotting using β-actin and GAPDH antibody. The detailed procedure is given in supplemental Materials and Methods.

Pull-down Assay—The detailed procedure is given in supplemental Materials and Methods.

Preparation of Nuclei and Nuclear Extract, Immunoblotting, Immunoprecipitation, and far-Western Blotting—For these techniques, the same procedure was followed as reported earlier (19). Nuclei were observed under a microscope (Fig. 1), and the purity of nuclear extract was checked by in-gel assay of MnSOD and immunoblotting by β-actin and GAPDH antibody. The detailed procedure is given in supplemental Materials and Methods.

MALDI-MS Analysis

The detailed procedure is given in supplemental Materials and Methods.

Identification of Putative Proteins

The detailed procedure is given in supplemental Materials and Methods.

Identification of Motifs

The detailed procedure is given in supplemental Materials and Methods. Briefly, the same procedure was followed as earlier reported (20).

Peptide Pull-down Assay

All the peptide sequences were purchased from GL Biochem Ltd, Shanghai, China. The peptide sequence from N to C ter-

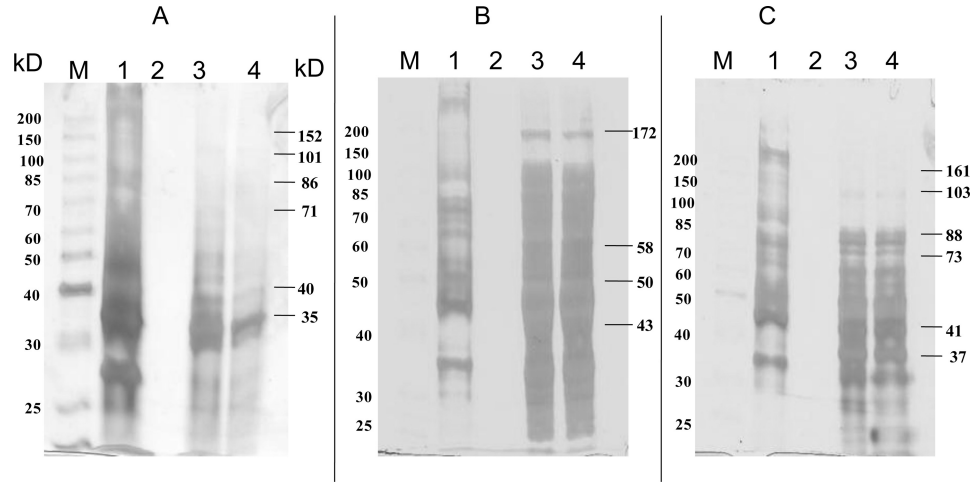

FIGURE 2. **Pull-down assay showing interaction of (*A*) ERβ, (*B*) TAD, and (*C*) LBD with mitochondrial proteins of the mouse brain.** Interacting prey proteins were resolved by SDS-PAGE, and detected by silver staining. *Lane M*: marker (Fermentas); *lane 1*: mitochondrial extract; *lane 2*: beads; *lane 3*: interacting proteins in the presence of estradiol; *lane 4*: interacting proteins in the absence of estradiol.

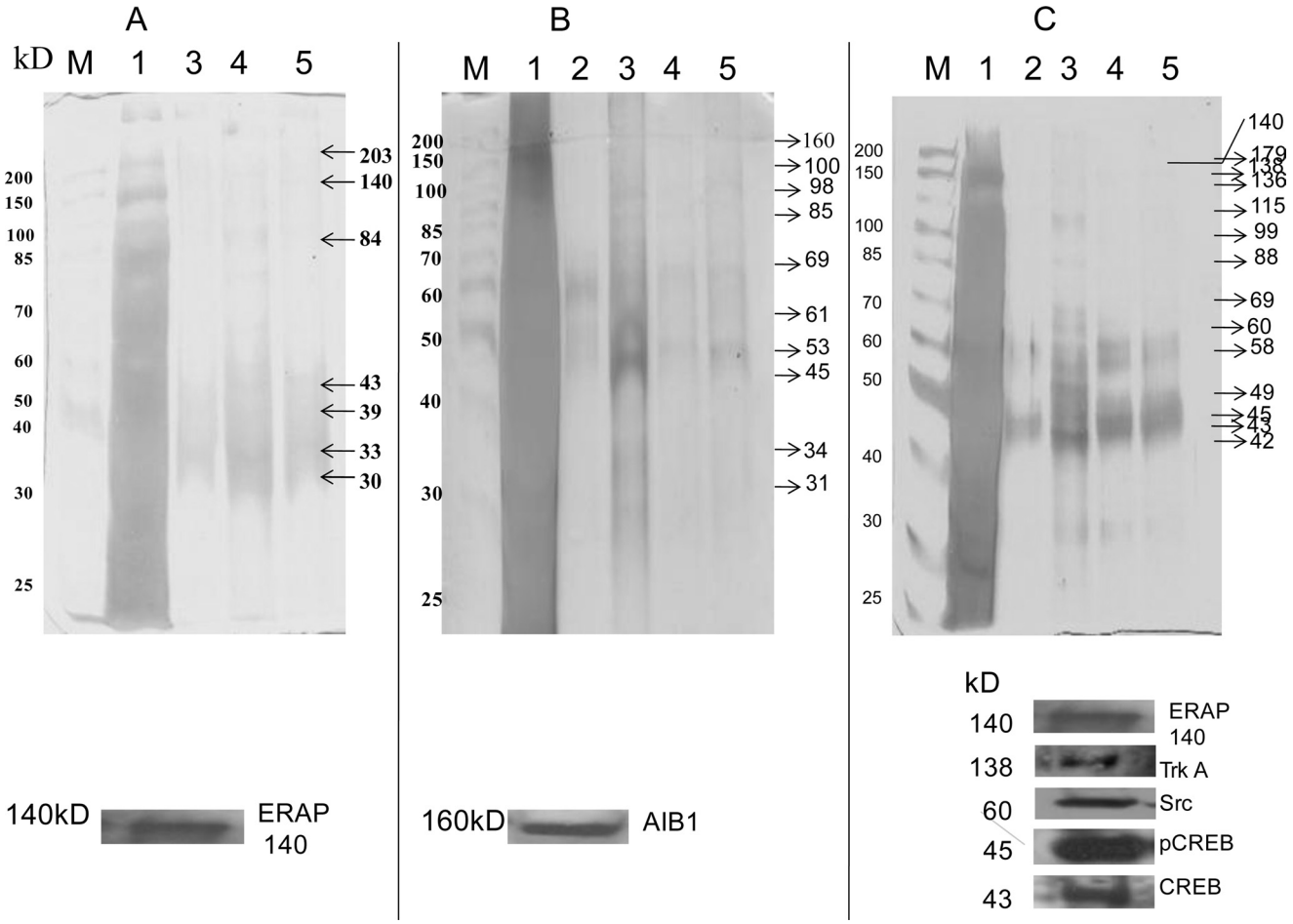

FIGURE 3. **Pull-down assay showing interaction of (*A*) ERβ, (*B*) TAD, and (*C*) LBD with nuclear proteins of mouse brain.** *Upper panel*: interacting prey proteins were resolved by SDS-PAGE, and detected by silver staining. *Lane M*: marker (Fermentas); *lane 1*: nuclear extract; *lane 2*: beads; *lane 3*: Eluate following interaction of His tag protein with nuclear extract; *lane 4*: interacting proteins in the absence of estradiol; *lane 5*: interacting proteins in the presence of estradiol. *Lower panel*: immuoblot analysis showing interacting proteins (present in *lane 5*) as ERAP 140, AIB 1, Trk A, Src, pCREB, and CREB.

minus; namely for (casein kinase) CK2: RRREDEESDDEEEA, mutated CK2: RRREDEEPPALEEEA, (phosphokinase) PKC: CRFARKGSLRQKNV, mutated PKC: CRFARKGPPAQKNV, *N*-myristoylation: RCRMGGFLATSLSW, and mutated *N*-myristoylation: RCRMAAIPLASLSW were used for the peptide pull-down assay. All the peptide sequences were biotin tagged at the N terminus. For the interaction study, CK2, PKC, and *N*-myristoylation sites and their respective mutants were used. Briefly, 1 mg of each peptide was dissolved in 1 ml and aliquoted. Avidin beads were purchased from Sigma, suspended

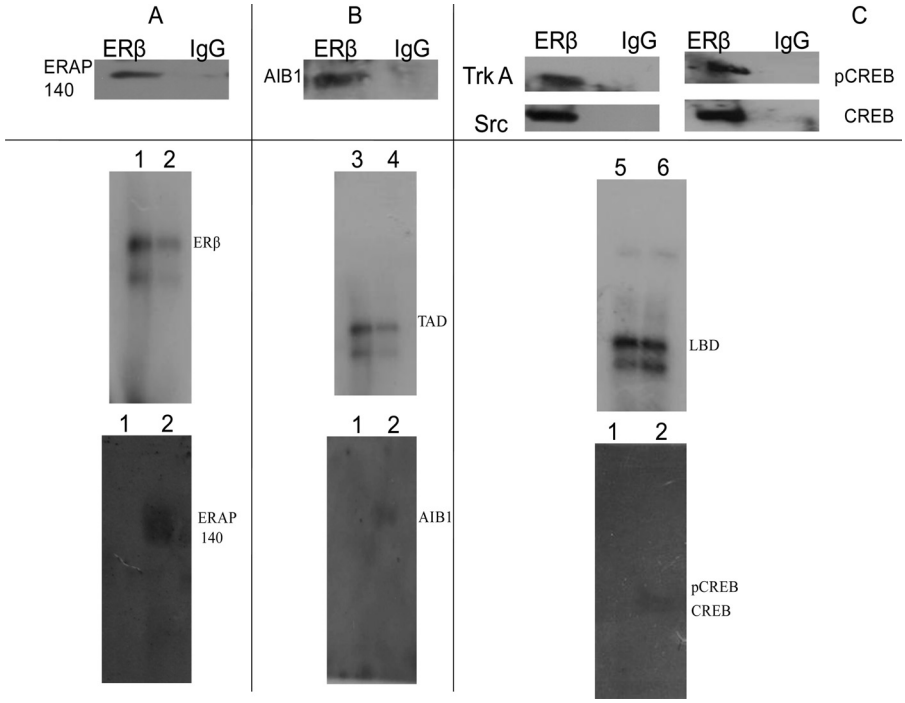

FIGURE 4. **Identification of (*A*) ERβ-, (*B*) TAD-, and (*C*) LBD-interacting proteins.** *Upper panel*, immunoprecipitation shows the interaction of ERAP 140 with ERβ, AIB1 with TAD and Trk A, Src, pCREB, and CREB with LBD. Briefly, nuclear extract from mouse brain was immunoprecipitated with anti-ERβ antibody, followed by immunoblotting with anti-ERAP 140, anti-AIB1, anti-Trk A, anti-Src, anti-pCREB, and CREB. *Middle panel: in vitro* labeling of fusion proteins and their purification. *Lane 1*: [^{35}S]methionine labeled ERβ with reaction mixture; *lane 2*: purified labeled ERβ; *lane 3*: γ-labeled [^{32}P]TAD reaction mixture; *lane 4*: purified labeled TAD; *lane 5*: γ-labeled [^{32}P]LBD with reaction mixture; *lane 6*: purified labeled LBD. *Lower panel*: identification of interacting proteins by far-Western blotting. *Lane 1*: bacterial extract (negative control) and *lane 2*: mouse brain nuclear extract (positive control) were resolved by SDS-PAGE and transferred onto membrane. Subsequently the blot was denatured/renatured and hybridized with (*A*) [^{35}S]methionine-labeled ERβ, (*B*) γ-labeled [^{32}P]TAD, and (*C*) γ-labeled [^{32}P]LBD, and signals were detected by autoradiography.

in 400 μl of 1× PBS, and incubated with 100 μg of biotinylated peptide overnight. Then it was washed three times with 1 ml of PBS to remove unbound peptides. Thereafter, 15 μl of washed peptide bound beads and 5 μg of purified ERβ, TAD, and LBD were incubated in 400 μl of binding buffer for 4 h at 4 °C. After incubation, the beads were washed with washing buffer three times. Then the beads-protein complex was resuspended in 40 μl of Laemmli buffer and boiled at 100 °C for 5 min. Finally, it was centrifuged at 10,000 × *g* for 5 min, the supernatant was resolved by 7.5% SDS-PAGE, and the band was detected by silver staining.

RESULTS AND DISCUSSION

Before conducting experiments using mitochondrial and nuclear fractions, the purity of these fractions was checked. The presence of MnSOD activity in the gel assay in the mitochondrial fraction and absence of GAPDH and β-actin by immunoblotting confirmed the purity of mitochondrial fraction (Fig. 1). Further, the absence of MnSOD activity by in-gel assay and the presence of β-actin and GAPDH by immunoblotting confirmed nuclear extract purity (Fig. 1).

Before performing the pull-down assay, we have analyzed the ERβ and its domains interacting proteins using bioinformatics tools (STRING 8.0, PIP, BIND, and DIP) and literature-based studies (iHOP, NCBI, and ISI web of knowledge). This showed several interacting partners of ERβ, but the pull-down assay revealed relatively lower numbers of proteins, 16 in the range of 30–172 kDa in mitochondria (Fig. 2) and 31 in the range of 31–203 kDa in the nuclei (Fig. 3).[3]

Surprisingly Timm44, a bonafide mitochondrial protein, was found in the nuclear fraction of mouse brain, whereas the nuclear pore complex 86 kDa protein was found in the mitochondrial fraction. Timm 44 crosses through the nuclear pore and attaches to the translocator proteins of nuclear membrane (21). Similarly, Selvam *et al.* (22) identified some of the nuclear pore complex binding proteins in the mitochondrial extract of rat kidney. Two steps were used for identifying the proteins using mascot search engines. In the first step, all the peptide peaks including intense ions 842.933, 1476.33 1941, and 2384.7 in Fig. 1*A*, 1123.9 in Fig. 1*C*, and 1123.9 in Fig. 1*D* were used. It provided a list of proteins with various mascot scores and best matched unique peptide sequences. In the second step, these unique sequences were used to make identification more stringent with the higher mascot score. Detailed procedures have been provided in supplemental Materials and Methods. Also, one excel file showing procedure has been provided in the supplemental data. Thus, the proteins identified were more stringent with higher mascot score and collated to brain functions.

[3] We have shown immunoblots from our earlier published papers in Figs. 3 and 4. These show immunoblots of AIB 1 from Biogerontology (DOI 10.1007/s10522-011-9330-y) and of Trk A and Src from Neurochemical Research (DOI 10.1007/s11064-011-0631-y).

FIGURE 5. **Aligned unique peptides of mitochondrial proteins showing CK2 (*red*, four in number and starts with S/T), PKC (*green*, three in number and starts with S/T), and myristoylation sites (*blue*, five in number and starts with *G*) represented by bold amino acids interacting with (*A*) ERβ, (*B*) TAD, and (*C*) LBD.**

Interaction with Mitochondrial Proteins

ERβ-interacting Proteins—ERβ showed interaction with six proteins of 152 kDa (prenylated protein-tyrosine phosphatase, peaks-36, unique peptides-11 and mascot score-149), 101 kDa (BC026557 similar to nucleoporin, peaks-29, unique peptides-11 and mascot score-153), 86 kDa (AK009187 similar to mitotic phosphoprotein, peaks-35, unique peptides-13 and mascot score-170), 71 kDa (phosphoinositol 3-phosphate-binding protein, peaks-26, unique peptides-22 and mascot score-190), 40 kDa (MKIAA1251 protein peaks-31, unique peptides-17 and mascot score-84), and 35 kDa (MUSACMHCA alpha cardiac myosin heavy chain peaks-31, unique peptides-14 and mascot score-56) (Fig. 2*A* and supplemental Table S1*A* and Fig. S1, *A–F*). The 152 kDa protein matches to a receptor-like transmembrane protein and causes dynamic tyrosine phosphorylation and dephosphorylation at serine/threonine and participates in many aspects of cellular, physiological and pathological processes (23). The 86 kDa protein is a member of nucleoporins, which constitute the nuclear pore complex and interacts with transiently associated nuclear transport factors (24). The 71 kDa protein recruits cytosolic proteins to specific membrane compartment and acts as a spatial regulator of many cellular processes including endocytic trafficking and membrane fusion (25). The 40 kDa protein is involved in G-protein signaling and vesicle trafficking. Its mRNA in mouse brain has long 3′-UTR, which increases with evolutionary age and organism complexity (26).

C

161kD (PKC:3, Myristyl:6)

1 RP**GTEQGQ**SEARVRGQWGP**GSQAAA**RGFFRLTTLPGWKTGQWGP**GSQAAA**RGFLLVCS**SG**
61 RRLDELSLSFCAPSVA**GGCAGA**TFVGFLLVC**SSG**RRP**GTEQGQ**SEARVLDELSLSFCAPS
121 VA**GGCAGA**TFRVRL **134**

103kD (CK2:7, Myristyl:3)

1 QLPSMKKEIE**SIKE**QLPSMKKFLDCPVGQLMLKYQKIYQKILWKVRYNTYTQTLRKMCHR
61 EAAVMLKASQPQGAEPRCASRAVEE**SGLE**SEGIFRLMLSNESLHPPSFSRSF**GLAETG**DL
121 **SVED**MKKIMSDVPEGVIRVHAPLLSKVSNSQASVDSSA**SMEE**FLREINRMLSNESLHPPS
181 FSRSVQFQALHLMVMALPDANRDMEVEDSG**GVVLTAY**HSHARSDTAQALMAFFNKVIANE
241 SKNMNLWNISTVMAPNLFFSRSKHTN**GSADAE**QSV**QSTL**SDDDYHGKNIRHL**SLIE**LTAF
301 FDTFGIQLKRDIFGVSESPPSDSCEHA**TQLD**GTKEGPDIKVQFQALHLMVMALPDANRDG
361 PDIKVQFQALHLMVMALPDANRD **383**

88kD (CK2:2, PKC:1, Myristyl:2)

1 CYPRREFNYVVRLRFLDEKSNFMNILEKVLCQYHF**SER**QWIYVHKG**STKE**TKTQYFHQEK
61 WREQYGVTLQLCKHNFMNILEKVVLKVSVLVGNINMWVYRMENLFSSLNYDVAAKKELLQ
121 TLYTSLCTLVQRV**GL**T**ITD**LPVCLQLNIMQRLFLDEKS**GSFVSD**LSSYCNKESQLTSLSG
181 IAQKNFMNILEKV **193**

73kD (CK2:5, PKC:3)

1 EKGPYRRRETLCRYTVTNVVRTMTVTNVVR**TTLE**QGM**TSKY**S**ITE**HIQERNVNNVVKPLH
61 KAYISEHIQERNAVISEN ITEHIQERDTVTNVVRTLEQGM**TSK**YNPMNV**TNVE**KPLQEGV
121 **TSK**NNPMNLTNVVKPLQEGV**TFKE**DNMNVTSMVKPLQEAVVSNAIKDNPMNVTTVVKPL
181 HKAVLSE**SISE**HIQERN **197**

41kD (CK2:2, PKC:4, Myristyl:5)

1 ENLG**GNSRTV**GREDAERRADST**GAKGTL**AASVS**SLHE**RIDSVLTWLLREI**SLVD**LA**GSER**
61 **AE**DG**GTLGVF**S**PK**KEALLAEMGVAMRECNAIINEDPNNKLVREHPLLGPYVEDL**SKLETE**
121 **KI**IAELNE**TWEE**KLLAVT**SYND**IQDLMDS**GNKATA**MVAAL**SPAD**INYDETLS**TLR**YADRA **180**

37kD (CK2:3, PKC:2, Myristyl:3)

1 LGATAEKAIFV**TSK**NGLVAEGHRLILGAVAKVREGEGESPQARATISPMVMDAKAAANFE
61 NHSGRL**STVE**G**IQASV**KTREVENSEDPKFSLLDASEEAIKKDAVAGNISDPDLQK**SSTVE**
121 **GIQASV**K**TARE**LGATAEKAAAVGTANKSLANVMMGPYRQDLLAKCAASDELSKTISPMVM
181 DAKAGLVAEGHRLANVMMGPYRQILLRNP**GNQAAY**EHFE**TMK**NCKVAMANIQPQMLVAGA
241 TSIARRVDQLTAQLADLAARGEGESPQARAMTGLVDEAIDTKSLLDASEEAIKK **294**

FIGURE 5—*continued*

TAD-interacting Proteins—TAD showed interaction with four proteins of 172 kDa (Abhd4 protein, peaks-32, unique peptides-13, and mascot score-160), 58 kDa (aldehyde reductase, peaks-29, unique peptides-17, and mascot score-199), 50 kDa (survival of motor neuron, peaks-31, unique peptides-4, and mascot score-42) and 43 kDa (AIG1 family/TONB Box N terminus, peaks-36, unique peptides-20, and mascot score-158) (Fig. 2*B* and supplemental Table S1*B* and Fig. S1, *G–J*). The 172 kDa protein is a lysophospholipase selective for *N*-acyl phosphatidylethanolamine (NAPE) and is involved in the biosynthesis of endocannabinoid anandamide by hydrolyzing the sn-1 and sn-2 acyl chains from NAPE generating glycerophospho-*N*-acyl ethanolamine (GP-NAE), an intermediate for *N*-acyl ethanolamine biosynthesis. It hydrolyzes substrates bearing saturated, monounsaturated, and polyunsaturated *N*-acyl chains. Its interaction with ERβ suggests the role of estrogen in the regulation of the cannabinoid receptor and neuroprotection against cannabinoids (27). The 58 kDa protein is aldo-keto reductase, which catalyzes a number of redox transformations of glucose, steroids, glycosylation end products, lipid peroxidation products and environmental pollutants involved in biosynthesis, intermediary metabolism, and detoxification. It plays an important role in the detoxification of a large number of pharmaceuticals, drugs, and xenobiotics (28). The 50 kDa protein binds to small actin-binding protein and is involved in snRNP transport and nuclear RNA splicing (29).

LBD-interacting Proteins—LBD interacted with six proteins of 161 kDa (E130112J05 product protein, peaks-36, unique peptides-7, and mascot score-126), 103 kDa (Arhgap28 protein, peaks-33, unique peptides-24 and mascot score-188), 88 kDa (AK014612, f-box only protein, peaks-33, unique peptides-15, and mascot score-162), 73 kDa (LOC433520 protein, peaks-32, unique peptides-9, and mascot score-92), 41 kDa (kinesin-related microtuble-based motor protein, peaks-32, unique peptides-13, and mascot score-62) and 37 kDa (vinculin, peaks-32, unique peptides-20 and mascot score-136) (Fig. 2*C* and supplemental Table S1*C* and Fig. S1, *K–P*). The 103 kDa protein is cytoskeletal and provides mechanical support to the plasma membrane and is involved in cell signaling, protein trafficking, control of cell proliferation, cell migration, adhesion, cytokinesis, and transcriptional activity (30). The 41 kDa is putatively identified as kinesins which are expressed in juvenile tissues including differentiated young neurons. Its expression is decreased considerably in adult mouse. It is involved in the transport of organelles through the axon, nucleotide-dependent binding to microtubules, microtubule-activated ATPase activity and microtubule plus-end-directed motility (31). The 37 kDa vinculin is a member of kinesin-like proteins (KLPs). It

FIGURE 6. **Aligned unique peptides of nuclear proteins showing CK2 (*red*, four in number and starts with S/T), PKC (*green*, three in number and starts with S/T), and myristoylation sites (*blue*, five in number and starts with *G*) represented by bold amino acids interacting with (*A*) ERβ, (*B*) TAD, and (*C*) LBD.**

is involved in the localization of the mitotic spindle and ATP hydrolysis to move along microtubules in a unidirectional manner, transporting chromosomes or other microtubules toward either the plus or minus end of the microtubule polymer (32).

Interaction with Nuclear Proteins

ERβ-interacting Proteins—ERβ interacted with seven putative proteins of 203, 140, 84, 43, 39, 33, and 30 kDa in mouse brain (Fig. 3*A* and supplemental Table 2*A* and Fig. S2, *A–F*). The 140 kDa protein was identified as estrogen receptor associated protein (ERAP) 140 by immunoblotting, immunoprecipitation, and far-Western blot analysis (Fig. 4*A*), and the remaining proteins by MALDI-MS. The variation in MW determined by pull-down and MALDI-MS analysis was due to their multisubunit characteristics and post-translational modifications, especially glycosylation.

The 203 kDa protein matches putatively to MKIAA1251 (peaks-20, unique peptides-22 and mascot score-109) and Ugcgl2 (peaks-20, unique peptides-13, and mascot score-104). The 140 kDa protein is characterized as a conserved tissue-specific nuclear receptor coactivator with abundant expression in brain, exclusively in neurons. Its homologues are present in both invertebrates as well as vertebrates including human (33). We recently reported that mouse ERβ interacts with estrogen receptor-associated protein (ERAP) 140 and shows variation in the levels of interaction and expression during aging of mouse brain (19). The 84 kDa protein matches to MMU10551(peaks-28, unique peptides-16 and mascot score-84), which is a member of the Ras superfamily and plays an important role in the regulation of L-type calcium channels and diverse cellular processes like cell growth, differentiation, cytoskeleton regulation, vesicular transport, cytokinesis, phagocytosis, pinocytosis, cell migration, morphogenesis, and axon guidance (34). The 43 kDa band matches to salivary androgen-binding protein (ABP) γ subunit fragment (peaks-25, unique peptides-7 and mascot score-63), which plays a role in sexual selection during brain development (35). The 39 kDa protein matches to adult male epididymis cDNA, RIKEN full-length enriched library, clone: 9230110G02 product: ATP/GTP-binding site motif A (P-loop)/zinc finger (peaks-25, unique peptides-19 and mascot score-183) (36). The 33 kDa protein matches to MMFXR1H9 (peaks-29, unique peptides-17, and mascot score-175), which is

FIGURE 6 —*continued*

present in the brain and shows estrogen dependent expression and regulation (37). The 30 kDa protein matches to adult male small intestine cDNA clone product, RIKEN full-length enriched library, clone:2010015J01 product:weakly similar to Arp2/3 complex 16 kDa subunit (P16-ARC, actin-related protein 2/3 complex subunit 5, peaks-18, unique peptides-12, and mascot score-156) which is present in the brain of fetal down syndrome patient and is responsible for neuronal and glial migration during brain development (38).

TAD-interacting Proteins—TAD interacted with ten proteins of 160, 100, 98, 85, 69, 61, 53, 45, 34, and 31 kDa (Fig. 3*B* and supplemental Table S2*B* and Fig. S2, *G–O*). The 160 kDa protein was identified as amplified in breast cancer (AIB) 1 by immunoblotting, immunoprecipitation, and far-Western blot analysis (Fig. 4*B*). AIB1 is a member of the nuclear coactivator (NCoA-3) and p160 steroid receptor co-activator (SRC) family, which includes SRC-1 and TIF-2 and plays a role in breast cancer and enhances angiogenesis and neurogenesis (39). We recently reported that mouse ERβ interacts with amplified in breast cancer (AIB) 1 (38) and showed variation in the levels of interaction and expression during aging of mouse brain. The 100 kDa protein is probably an iron-binding protein P97 (peaks-31, unique peptides-8, and mascot score-127), but its physiological role is not clear in brain. Originally, it was discovered in melanoma cells, but now it is known to be expressed at varying levels in several kinds of tumors. In normal tissues, it is expressed at high levels in fetal gut, adult sweat gland, and probably brain capillaries. P97 is structurally homologous to transferrin and is shown to bind to iron and zinc. It is reported as a marker in Alzheimer patients, which show its elevated level in serum (40). The 98 kDa protein is identified as an adult inner ear protein (peaks-20, unique peptides-6, and mascot score-113), which is a member of Nkx5–1 family and has various roles in inner ear and hindbrain development (42). The 85 kDa protein matches to MKIAA 0670 (peaks-24, unique peptides-23, and mascot score-139), which is a member of KIAA family with unknown biological function (43). The 69 kDa protein has been identified as 18th day whole body protein (peaks-26, unique peptides-9, and mascot score-112), and acts as a homeodomain transcription factor in brain. The 61 kDa protein is a ankyrin protein (peaks-31, unique peptides-19 and mascot score-187), expressed in brain and plays a vital role in energy homeostasis (44). The 53 kDa protein is identified as bone marrow macrophage tRNA synthetase (peaks-35, unique peptides-22, and mascot score-192). The 45 kDa protein matches to melanocyte protein (peaks-26, unique peptides-22, and mascot score-207) known for induction of melanocyte-stimulating hormone and its related function in neurons (45). The 34 kDa protein

C

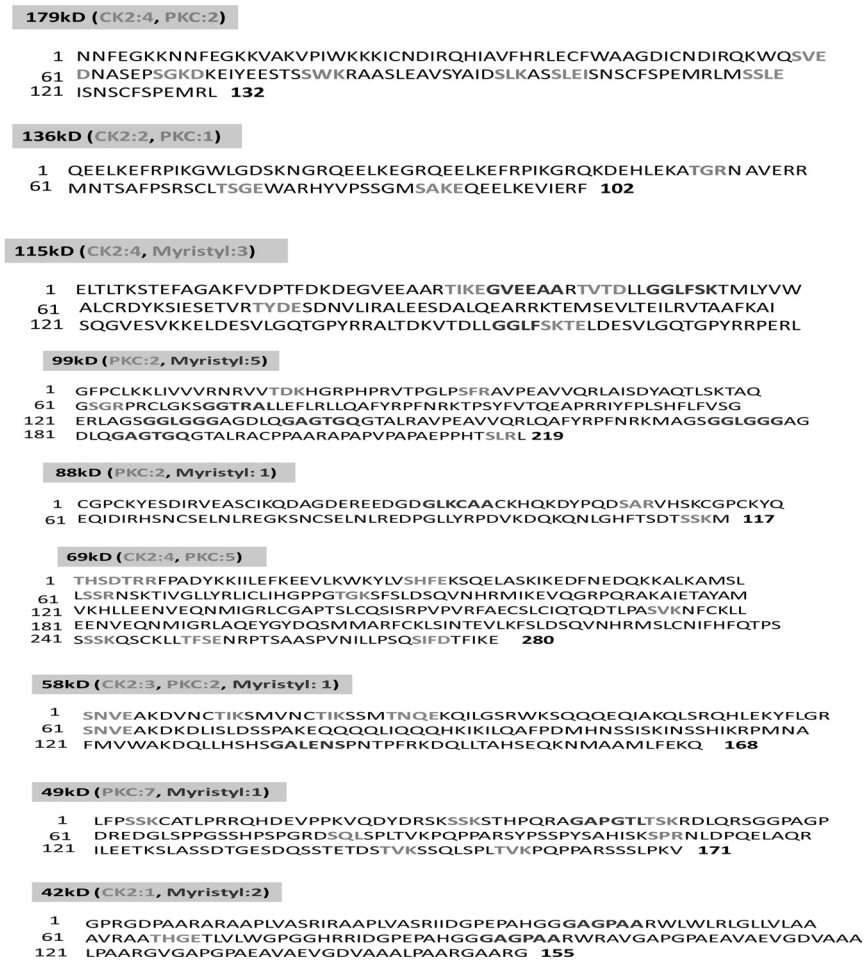

FIGURE 6 —*continued*

matches to caldesmon (peaks-29, unique peptides-17, and mascot score-150), binds to actin and calmodulin. It accumulates in the post-synaptic densities of asymmetric synapses and is involved in the actin-linked regulation of smooth muscle and non-muscle myosin II ATPase activity and polymerization of cytoskeleton proteins. The 31 kDa protein is identified as an adult bone marrow protein, (peaks-22, unique peptides-13, and mascot score-139) and plays an important role in cell proliferation during development.

LBD-interacting Proteins—LBD interacted with 14 proteins of 179, 140, 138, 136, 115, 99, 88, 69, 60, 58, 49, 45, 43, and 42 kDa (Fig. 3*C* and supplemental Table S2*C* and Fig. S2, *P–X*). Among them 140, 138, 60, 45, and 43 kDa were identified as ERAP 140, TrkA, Src, pCREB, and cAMP response element binding protein (CREB), respectively, by immunoblotting, immunoprecipitation, and far-Western blot analysis (Fig. 4*C*).

The 179 kDa protein has been identified as a molydopterin converting factor subunit 2 containing protein (peaks-24, unique peptides-12, and mascot score-163), and functions as a cofactor in metabolic activity (46). The 138 kDa protein is Trk A, which is known for the autophosphorylation and recruitment of signaling molecules and activates a receptor-specific intracellular signaling pathway that relays information to nucleus and other intracellular compartments (47). The 136 kDa protein is identified as 2nd day oviduct protein (peaks-21, unique peptides-12 and mascot score-122), and has no well known function. The 115 kDa protein is Tim 44 (peaks-18, unique peptides-15, and mascot score-137), which is responsible for the transportation of proteins to membrane and suborganelles including mitochondria. It controls the oxidative phosphorylation and takes part in the respiratory chain enzyme kinetics (48). The 99 kDa protein is heparan sulfate sulfotransferase isoform 6 (peaks-29, unique peptides-16, and mascot score-182), and is reported in the brain. The 88 kDa protein matches to tomoregulin (peaks-16, unique peptides-13, and mascot score-140), and is a transmembrane protein predominantly expressed in the brain. The 69 kDa protein has been identified as senataxin (peaks-23, unique peptides-21, and mascot score-70), which causes a rare juvenile-onset form of amyotrophic lateral sclerosis (ALS). The 58 kDa matches to SRY protein (peaks-24, unique peptides-14, and mascot score-127), known as the key sex-determining protein that directs gonads to develop as testes rather than ovaries. The 60 kDa protein is identified as Src which belongs to a family of highly homologous proteins with protein tyrosine kinase (PTK) activity and resides in the cytoplasm and perinuclear space. Recent reports suggest that Src is also located at the plasma membrane and several subcellular compartments including the nucleus (49) and involves in signal transduction. The 49 kDa protein has been identified as a member of KIAA gene family (peaks-23,

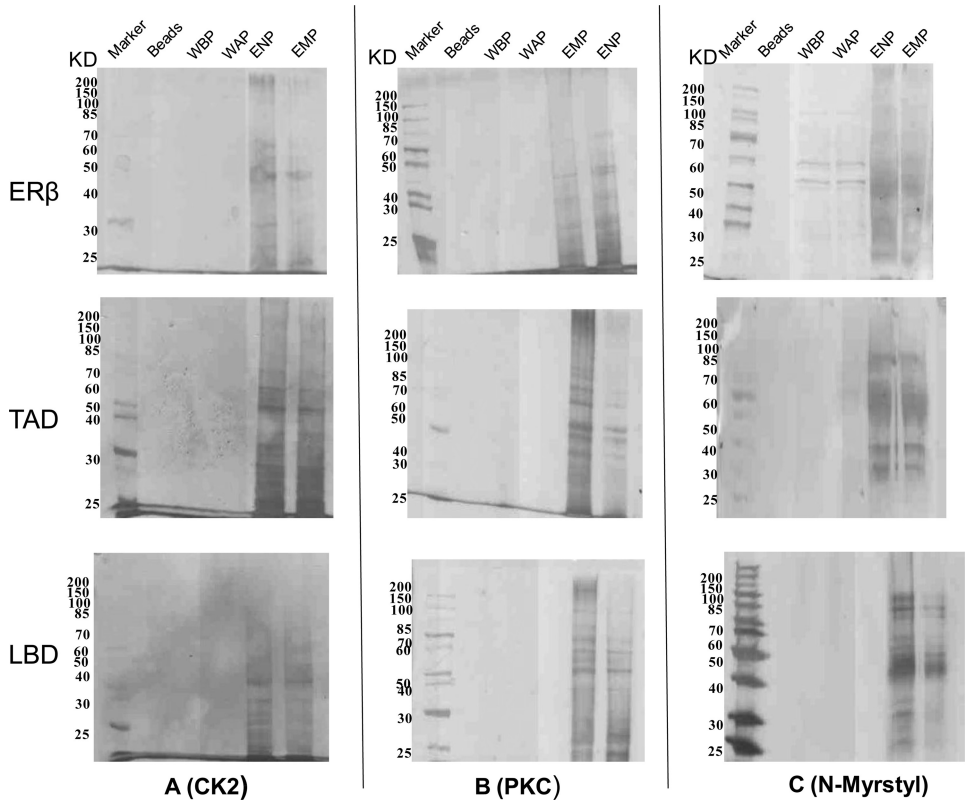

FIGURE 7. **Peptide pull-down assay showing interaction of (*upper panel*) ERβ, (*middle panel*) TAD, and (*lower panel*) LBD with peptides containing CK2 (*A*), PKC (*B*), and *N*-myristoylation sites (*C*) and their respective mutations.** The pulled-down proteins were resolved by SDS-PAGE, and detected by silver staining. *Lane M*: marker (Fermentas); *lane 1*: beads; *lane 2*: wash before binding of proteins (*WBP*); *lane 3*: wash after binding of proteins (*WAP*); *lane 4*: eluate showing proteins interacting with normal peptides (ENP); *lane 5*: eluate showing proteins interacting with mutated peptides (*EMP*).

unique peptides-13, and mascot score-118), and its role in brain function is not clear (41). The 45 kDa and 43 kDa proteins have been identified as pCREB and CREB, respectively. They are well known transcription factors involved in multiple brain functions. Moreover, 42 kDa protein is identified as alanine region protein (peaks-29, unique peptides-9, and mascot score-123), and is known for its role in signal transduction in the brain (50).

Identification of Consensus Motifs

As all the mitochondrial and nuclear proteins interacted with ERβ and its domains, we assume that these proteins have a common consensus binding motifs. Therefore, all the interacting proteins were analyzed by motif scan, and interestingly they were found to contain consensus motifs CK2, PKC phosphorylation, and *N*-myristoylation sites (Fig. 5 and Fig. 6). This was also confirmed by peptide pull-down assay using specific biotinylated CK2, PKC, and *N*-myristoylation peptides. CK2, PKC phosphorylation and *N*-myristoylation sites showed interaction with ERβ, TAD and LBD whereas no interaction was observed with their respective mutants (Fig. 7). The gels show the binding difference between normal and mutated peptides with ERβ and its domains. In string 8.0, peptide sequences did not show any match with putative proteins. So it is likely that these are bacterial proteins contaminations. Both CK2 and PKC phosphorylation sites start with serine or threonine residue, and phosphorylation at these sites is responsible for the interaction of all the putatively identified proteins with ERβ resulting in the downstream functions, namely neuronal architecture, migration of neuronal and glial cells during development and cell proliferation (51). Further, *N*-myristoylation is involved in the anchoring of proteins and their targeting to cell membrane and plays a critical role in cell signaling, apoptosis and extracellular protein export. The myristoyl-CoA and *N*-myristolyltransferase (NMT) recognize the sequence motif of myristate site at N-terminal glycine residues. Apart from anchoring, myristoylation is also involved in the docking of Ca^{2+} (52).

As protein interactions are transient, our proteomic approach precisely analyzes the interacting proteins by pull-down assay followed by MALDI-MS and identifies their motifs by motif scan software. The identification of ERβ-interacting proteins in brain mitochondria indicates the importance of ERβ in the regulation of mitochondrial gene expression. This is contradictory to an earlier observation in which ERβ was reported as a poor transcription factor (53, 54). The present study is of great significance as it advances our knowledge of nuclear receptor and its interaction and functional analysis in the brain mitochondria. The putatively identified proteins are involved in cellular signaling in mitochondria. The reduced level of putatively identified survival motor neuron (SMN) protein causes spinal muscular atrophy. The CK2, PKC, and *N*-myristoylation sites have been identified for the first time as consensus motifs in all ERβ interacting proteins in the brain mitochondria. This raises the possibility to regulate the estro-

gen dependent gene expression through ERβ in health and disease (10).

Taken together, our studies showed that ERβ and its domains interact with the consensus CK2, PKC phosphorylation, and *N*-myristoylation sites of specific mitochondrial as well as nuclear proteins. Evidences from literature suggest that these interacting proteins are involved in neuronal architecture, cytoskeleton integrity, signal transduction, and cell proliferation. The identification of consensus binding motifs in ERβ-interacting proteins of the brain mitochondria represents an essential step toward designing selective ER modulators for understanding estrogen-mediated signaling.

Acknowledgments—We thank Prof. Vincent Giguere for providing the plasmid pCMX-mouse ERβ as a kind gift, and Prof. J. A. Gustafsson for suggestions to prepare the manuscript.

REFERENCES

1. Kato, S., Sato, T., Watanabe, T., Takemasa, S., Masuhiro, Y., Ohtake, F., and Matsumoto, T. (2005) Function of nuclear sex hormone receptors in gene regulation. *Cancer Chemother. Pharmacol.* **56,** 4–9
2. Hall, J. M., Couse, J. F., and Korach, K. S. (2001) The multifaceted mechanisms of estradiol and estrogen receptor signaling. *J. Biol. Chem.* **276,** 36869–36872
3. Levin, E. R. (2005) Integration of the extranuclear and nuclear actions of estrogen. *Mol. Endocrinol.* **19,** 1951–1959
4. Song, R. X., and Santen, R. J. (2006) Membrane initiated estrogen signaling in breast cancer. *Biol. Reprod.* **75,** 9–16
5. Yang, S. H., Liu, R., Perez, E. J., Wen, Y., Stevens, S. M., Jr., Valencia, T., Brun-Zinkernagel, A. M., Prokai, L., Will, Y., Dykens, J., Koulen, P., and Simpkins, J. W. (2004) Mitochondrial localization of estrogen receptor β. *Proc. Natl. Acad. Sci. U.S.A.* **101,** 4130–4135
6. Chen, J. Q., Delannoy, M., Cooke, C., and Yager, J. D. (2004) Mitochondrial localization of ERα and ERβ in human MCF7 cells. *Am. J. Physiol. Endocrinol. Metab.* **286,** E1011–E1022
7. Oñate, S. A., Tsai, S. Y., Tsai, M. J., and O'Malley, B. W. (1995) Sequence and characterization of a coactivator for the steroid hormone receptor superfamily. *Science* **270,** 1354–1357
8. Hong, H., Kohli, K., Trivedi, A., Johnson, D. L., and Stallcup, M. R. (1996) GRIP1, a novel mouse protein that serves as a transcriptional coactivator in yeast for the hormone binding domains of steroid receptors. *Proc. Natl. Acad. Sci. U.S.A.* **93,** 4948–4952
9. Voegel, J. J., Heine, M. J., Zechel, C., Chambon, P., and Gronemeyer, H. (1996) TIF2, a 160 kDa transcriptional mediator for the ligand-dependent activation function AF-2 of nuclear receptors. *EMBO J.* **15,** 3667–3675
10. Thakur, M. K., and Paramanik, V. (2009) Role of steroid hormone coregulators in health and disease. *Horm. Res.* **71,** 194–200
11. Klein, F. A., Atkinson, R. A., Potier, N., Moras, D., and Cavarelli, J. (2005) Biochemical and NMR mapping of the interface between CREB-binding protein and ligand binding domains of nuclear receptor: beyond the L*XX*LL motif. *J. Biol. Chem.* **280,** 5682–5692
12. Chen, D., Huang, S. M., and Stallcup, M. R. (2000) Synergistic, p160 coactivator-dependent enhancement of estrogen receptor function by CARM1 and p300. *J. Biol. Chem.* **275,** 40810–40816
13. Shao, G., Heyman, R. A., and Schulman, I. (2000) Three amino acids specify coactivator choice by retinoid X receptors. *Mol. Endocrinol.* **14,** 1198–1209
14. Heinzel, T., Lavinsky, R. M., Mullen, T. M., Söderstrom, M., Laherty, C. D., Torchia, J., Yang, W. M., Brard, G. S., Davie, J. R., Seto E, Eisenman, R. N., Rose, D. W., Glass, C. K., and Rosenfeld, M. G. (1997) A complex containing N-CoR, mSin3 and histone deacetylase mediates transcriptional repression. *Nature* **387,** 43–48
15. Nagy, L., Kao, H. Y., Chakravarti, D., Lin, R. J., Hassig, C. A., Ayer, D. E., Schreiber, S. L., and Evans, R. M. (1997) Nuclear receptor repression mediated by a complex containing SMRT, mSin3A, and histone deacetylase. *Cell* **89,** 373–380
16. Paramanik, V., and Thakur, M. K. (2010) Overexpression of mouse estrogen receptor-β decreases but its transactivation and ligand binding domains increase the growth characteristics of *E. coli*. *Mol. Biotechnol.* 47, 26–33
17. Paramanik, V., and Thakur, M. K. (2011) NMR analysis reveals 17β-estradiol induced conformational change in ERβ ligand binding domain expressed in *E. coli*. *Mol. Biol. Rep.* **38,** 4657–4661
18. Kudin, A. P., Bimpong-Buta, N. Y., Vielhaber, S., Elger, C. E., and Kunz, W. S. (2004) Characterization of superoxide-producing sites in isolated brain mitochondria. *J. Biol. Chem.* **279,** 4127–4135
19. Paramanik, V., and Thakur, M. K. (2010) Interaction of Estrogen Receptor Associated Protein (ERAP) 140 with ER β decreases but its expression increases in aging mouse cerebral cortex. *Cell Mol. Neurobiol.* 30, 961–966
20. Hulo, N., Bairoch, A., Bulliard, V., Cerutti, L., Cuche, B. A., de Castro, E., Lachaize, C., Langendijk- Genevaux, P. S., and Sigrist, C. J. (2008) The 20 years of PROSITE. *Nucleic Acids Res.* **36,** D245–D249
21. Kucej, M., Kucejova, B., Subramanian, R., Chen, X. J., and Butow, R. A. (2008) Mitochondrial nucleoids undergo remodeling in response to metabolic cues. *J. Cell Sci.* **121,** 1861–1868
22. Selvam, R., Vijaya, R., and Sivakamasundari P. (2003) Characterization of nuclear pore complex oxalate-binding protein from human kidney. *Mol. Cell Biochem.* **243,** 1–8
23. Streuli, M. (1996) Protein-tyrosine phosphatases in signaling. *Curr. Opin. Cell Biol.* **8,** 182–188
24. Stukenberg, P. T., Lustig, K. D., McGarry, T. J., King, R. W., Kuang, J. and Kirschner, M. W. (1997) Systematic identification of mitotic phosphoproteins. *Curr. Biol.* **7,** 338–348
25. Vanhaesebroeck, B., Leevers, S. J., Ahmadi, K., Timms, J., Katso, R., Driscoll, P. C., Woscholski, R., Parker, P. J., and Waterfield, M. D. (2001) Synthesis and function of 3-phosphorylated inositol lipids. *Annu. Rev. Biochem.* **70,** 535–602
26. Mazumder, B., Seshadri, V., and Fox, P. L. (2003) Translational control by the 3′-UTR: the ends specify the means. *Trends Biochem. Sci.* **28,** 91–98
27. McPartland, J. M., Norris, R. W., and Kilpatrick, C. W. (2007) Coevolution between cannabinoid receptors and endocannabinoid ligands. *Gene* **397,** 126–135
28. Barski, O. A., Tipparaju, S. M., and Bhatnagar, A. (2008) The aldo-keto reductase superfamily and its role in drug metabolism and detoxification. *Drug Metabol. Rev.* 40, 553–624
29. Sharma, A., Lambrechts, A., Hao le, T., Le, T. T., Sewry, C. A., Ampe, C., Burghes, A. H., and Morris, G. E. (2005) A role for complexes of survival of motor neurons (SMN) protein with gemins and profilin in neurite-like cytoplasmic extensions of cultured nerve cells. *Exp. Cell Res.* **309,** 185–197
30. Gascard, P., and Mohandas, N. (2000) New insights into functions of erythroid proteins in nonerythroid cells. *Curr. Opin. Hematol.* **7,** 123–129
31. Zhu, C., Zhao, J., Bibikova, M., Leverson, J. D., Bossy-Wetzel, E., Fan, J. B., Abraham, R. T., and Jiang, W. (2005) Functional analysis of human microtubule-based motor proteins, the kinesins and dyneins, in mitosis/cytokinesis using RNA interference. *Mol. Biol. Cell* **16,** 3187–3199
32. Pfarr, C. M., Coue, M., Grissom, P. M., Hays, T. S., Porter, M. E., and McIntosh, J. R. (1990) Cytoplasmic dynein is localized to kinetochores during mitosis. *Nature* **345,** 263–265
33. Shao, W., Halachmi, S., and Brown, M. (2002) ERAP140, a conserved tissue-specific nuclear receptor coactivator. *Mol. Cell Biol.* **22,** 3358–3372
34. Béguin, P., Nagashima, K., Gonoi, T., Shibasaki, T., Takahashi, K., Kashima, Y., Ozaki, N., Geering, K., Iwanaga, T., and Seino, S. (2001) Regulation of Ca^{2+} channel expression at the cell surface by the small G-protein kir/Gem. *Nature* **411,** 701–706
35. Karn, R. C., and Laukaitis, C. M. (2003) Characterization of two forms of mouse salivary androgen-binding protein (ABP): implications for evolutionary relationships and ligand-binding function. *Biochemistry* **42,** 7162–7170
36. Carninci, P., and Hayashizaki, Y. (1999) High-efficiency full-length cDNA cloning. *Methods Enzymol.* **303,** 19–44
37. Singh, K., and Prasad, S. (2008) Age- and sex-related analysis of methylation of 5′-upstream sequences of Fmr-1 gene in mouse brain and modu-

lation by sex steroid hormones. *Biogerontology* **9,** 455–465
38. de Hostos, E. L. (1999) The coronin family of actin-associated proteins. *Trends Cell Biol.* **9,** 345–350
39. Anzick, S. L., Kononen, J., Walker, R. L., Azorsa, D. O., Tanner, M. M., Guan, X. Y., Sauter, G., Kallioniemi, O. P., Trent, J. M., and Meltzer, P. S. (1997) AIB1, a steroid receptor coactivator amplified in breast and ovarian cancer. *Science* **277,** 965–968
40. Paramanik, V., and Thakur, M. K. (2011) AIB1 shows variation in interaction with ERβTAD and expression as a function of age in mouse brain. *Biogerontology* **12,** 321–328
41. Wilhelm, D., Palmer, S., and Koopman, P. (2007) Sex determination and gonadal development in mammals. *Physiol. Rev.* **87,** 1–28
42. Hadrys, T., Braun, T., Rinkwitz-Brandt, S., Arnold, H. H., and Bober, E. (1998) Nkx5-1 controls semicircular canal formation in the mouse inner ear. *Development* **125,** 33–39
43. Okazaki, N., Kikuno, R., Ohara, R., Inamoto, S., Aizawa, H., Yuasa, S., Nakajima, D., Nagase, T., Ohara, O., and Koga, H. (2003) Prediction of the coding sequences of mouse homologues of KIAA gene: II. The complete nucleotide sequences of 400 mouse KIAA-homologous cDNAs identified by screening of terminal sequences of cDNA clones randomly sampled from size-fractionated libraries. *DNA Res.* **10,** 35–48
44. Li, Y., Reznichenko, M., Tribe, R. M., Hess, P. E., Taggart, M., Kim, H. R., DeGnore, J. P., Gangopadhyay, S., and Morgan, K. G. (2009) Stretch activates human myometrium via ERK, caldesmon, and focal adhesion signaling. *PLoS One* **16,** e7489
45. Kubota, R., Wang, Y., Minoshima, S., Kudoh, J., Mashima, Y., Oguchi, Y., and Shimizu, N. (1995) Mapping of the human gene for a melanocyte protein Pmel 17 (D12S53E) to chromosome 12q13-q14. *Genomics* **26,** 430–431
46. Reiss J, Dorche, C., Stallmeyer, B., Mendel, R. R., Cohen, N., and Zabot, M. T. (1999) Human molybdopterin synthase gene: genomic structure and mutations in molybdenum cofactor deficiency type B. *Am. J. Hum. Genet.* **64,** 706–711
47. Schlesinger, J. (2000) Cell signaling by receptor tyrosine kinases. *Cell* **103,** 211–225
48. Schiller, D., Cheng, Y. C., Liu, Q., Walter, W., and Craig, E. A. (2008) Residues of Tim44 involved in both association with the translocon of the inner mitochondrial membrane and regulation of mitochondrial Hsp70 tethering. *Mol. Cell Biol.* **28,** 4424–4433
49. Takahashi, H., Suzuki, K., and Namiki, H. (2004) Pervanadate-induced reverse translocation and tyrosine phosphorylation of phorbol ester-stimulated protein kinase C βII are mediated by Src-family tyrosine kinases in porcine neutrophils. *Biochem. Biophys. Res. Commun.* **314,** 830–837
50. Kyriaris, J. M., and Avruch, J. (2001) Mammalian mitogen-activated protein kinase signal transduction pathways activated by stress and inflammation. *Physiol. Rev.* **81,** 807–869
51. Ohmori, S., Sakai, N., Shirai, Y., Yamamoto, H., Miyamoto, E., Shimizu, N., and Saito, N. (2000) Importance of protein kinase C targeting for the phosphorylation of its substrate, myristoylated alanine-rich C-kinase substrate. *J. Biol. Chem.* **275,** 26449–26457
52. Maurer-Stroh, S., Eisenhaber, B., and Eisenhaber, F. (2002) N-terminal *N*-myristoylation of proteins: refinement of the sequence motif and its taxon-specific differences. *J. Mol. Biol.* **317,** 523–540
53. Pettersson, K., Grandien, K., Kuiper, G. G., and Gustafsson, J. A., (1997) Mouse estrogen receptor β forms estrogen response element-binding heterodimers with estrogen receptor alpha. *Mol. Endocrinol.* **11,** 1486–1496
54. Cowley, S. M., Hoare, S., Mosselman, S., and Parker, M. G., (1997) Estrogen receptors α and β form heterodimers on DNA. *J. Biol. Chem.* **272,** 19858–19862